Controlo 2002

5th Portuguese Conference on Automatic Control

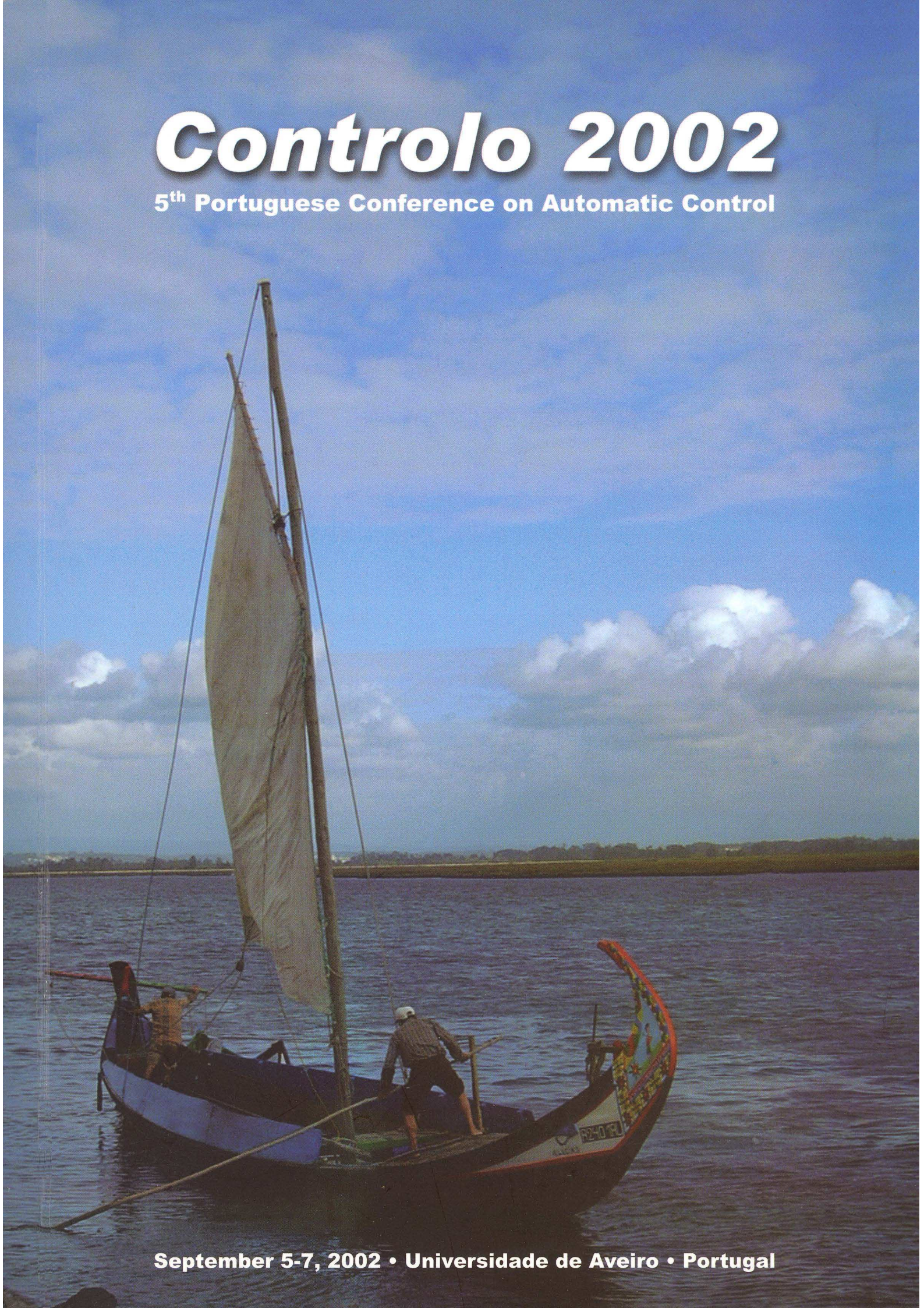

September 5-7, 2002 • Universidade de Aveiro • Portugal

Proceedings of Controlo 2002
5th Portuguese Conference on Automatic Control
Aveiro, Portugal, September 5-7, 2002

A FRACTIONAL CALCULUS PERSPECTIVE OF MECHANICAL SYSTEMS MODELING

R. S. Barbosa * F. B. M. Duarte ** J. A. T. Machado *

** Department of Electrotechnical Engineering*
Institute of Engineering of Porto, Portugal
E-mail: {rbarbosa,jtm}@dee.isep.ipp.pt
*** Department of Mathematics*
School of Technology of Viseu, Portugal
E-mail: fduarte@mat.estv.ipv.pt

Abstract: The area of Fractional Calculus (FC) goes back to the beginning of the theory of differential calculus. Nevertheless, the application of FC just emerged in the last two decades, due to the progress in the area of chaos that revealed subtle relationships with the FC concepts. In the area of dynamical systems theory some work has been carried out but the proposed models and algorithms are still in a preliminary stage of establishment. Having these ideas in mind, the paper discusses a FC perspective in the study of the dynamics and control of mechanical systems. *Copyright © Controlo 2002*

Keywords: Fractional-Order Systems, Fractional Calculus, Mechanical Systems, Modeling.

1. INTRODUCTION

The generalization of the concept of derivative $D^{\alpha}f(x)$ to non-integer values of α goes back to the beginning of the theory of differential calculus. In fact, Leibniz, in his correspondence with Bernoulli, L'Hôpital and Wallis (1695), had several notes about the calculation of $D^{1/2}f(x)$. Nevertheless, the development of the theory of Fractional Calculus (FC) is due to the contributions of many mathematicians such as Euler, Liouville, Riemann and Letnikov (Oldham and Spanier, 1974; Miller and Ross, 1993). In the fields of physics and chemistry, FC is presently associated with the modeling of electro-chemical reactions, irreversibility and electromagnetism (Hilfer, 2000). The adoption of the FC in control algorithms has been recently studied (Machado, 1997; Machado, 2001; Oustaloup, 1995; Podlubny, 1999) using the frequency and discrete-time domains. Nevertheless, this research is still giving its first steps and further investigation is required.

This article introduces the fundamental aspects of the theory of FC and presents novel results on the dynamics and control of mechanical systems. In this perspective, the paper is organized as follows. Section 2 outlines the fundamental aspects of the theory of FC and its application in control theory. Section 3 presents several case studies on the implementation of FC-based models in the analysis and control of mechanical systems. Finally, section 4 draws the main conclusions.

2. FUNDAMENTAL ASPECTS OF THE THEORY OF FRACTIONAL CALCULUS

Since the foundation of the differential calculus the generalization of the concept of differentiation and integration to a non-integer order α has been the subject of several approaches. Due to this reason there are various definitions of fractional integrals and derivatives which are proved to be equivalent (Table 1). Nevertheless, the problem of devising and implementing fractional-order algorithms is not trivial.

In the last decade were proposed two methods for implementing fractional-order derivatives, namely the frequency-based and the discrete-time approaches.

Table 1 Some definitions of fractional integrals and derivatives

Riemann-Liouville	$\left(I_{a+}^{\alpha}\varphi\right)(x)=\frac{1}{\Gamma(\alpha)}\int_a^x\frac{\varphi(t)}{(x-t)^{1-\alpha}}dtt,\ a<x$
	$\left(D_{a+}^{\alpha}\varphi\right)(x)=\frac{1}{\Gamma(1-\alpha)}\frac{d}{dx}\int_a^x\frac{\varphi(t)}{(x-t)^{\alpha}}dt,\ a<x$
Grünwald-Letnikov	$\left(I_{a+}^{\alpha}\varphi\right)(x)=\frac{1}{\Gamma(\alpha)}\lim_{h\to+0}\left[h^{\alpha}\sum_{j=0}^{[(x-a)/h]}\frac{\Gamma(\alpha+j)}{\Gamma(j+1)}\varphi(x-jh)\right]$
Laplace	$L\left\{I_{0+}^{\alpha}\varphi\right\}=L\{\varphi\}/s^{\alpha},\ \mathrm{Re}(\alpha)>0$
	$L\left\{D_{0+}^{\alpha}\varphi\right\}=s^{\alpha}L\{\varphi\},\ \mathrm{Re}(\alpha)\geq 0$

In order to analyze a frequency-based approach to D^{α}, $0 < \alpha < 1$, let us consider the recursive circuit represented on Fig. 1 such that:

$$I = \sum_{i=0}^{n} I_i \,,\; R_{i+1} = \frac{R_i}{\varepsilon} \,,\; C_{i+1} = \frac{C_i}{\eta} \qquad (1)$$

where η and ε are scale factors, I is the current due to an applied voltage V and R_i and C_i are the resistance and capacitance elements of the i^{th} branch of the circuit.

The admittance $Y(j\omega)$ is given by:

$$Y(j\omega) = \frac{I(j\omega)}{V(j\omega)} = \sum_{i=0}^{n} \frac{j\omega C \varepsilon^i}{j\omega CR + (\eta\varepsilon)^i} \qquad (2)$$

Figure 2 shows the asymptotic Bode diagrams of amplitude and phase of $Y(j\omega)$. The pole and zero frequencies (ω_i and ω_i') obey the recursive relationships:

$$\frac{\omega_{i+1}'}{\omega_i'} = \frac{\omega_{i+1}}{\omega_i} = \varepsilon\eta \,,\; \frac{\omega_i}{\omega_i'} = \varepsilon \,,\; \frac{\omega_{i+1}'}{\omega_i} = \eta \qquad (3)$$

From the Bode diagram of amplitude or of phase, the average slope m' can be calculated as:

$$m' = \frac{\log \varepsilon}{\log \varepsilon + \log \eta} \qquad (4)$$

The fractional order of the frequency response is due to the recursive nature of the circuit. Consequently, the circuit of Fig. 1 represents an approach to D^{α}, $0 < \alpha < 1$, with $m' = \alpha$, based on a recursive pole/zero placement.

As mentioned previously, the Laplace definition for a derivative of order $\alpha \in C$ is a 'direct' generalization of the classical integer-order scheme with the multiplication of the signal transform by the s operator. Therefore, in what concerns automatic control theory this means that frequency-based analysis methods have a straightforward adaptation to their fractional-order counterparts.

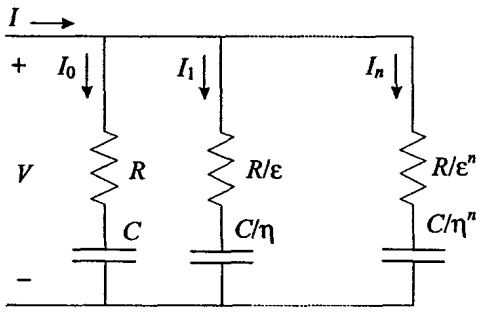

Fig. 1. Electrical circuit with a recursive association of resistance and capacitance elements.

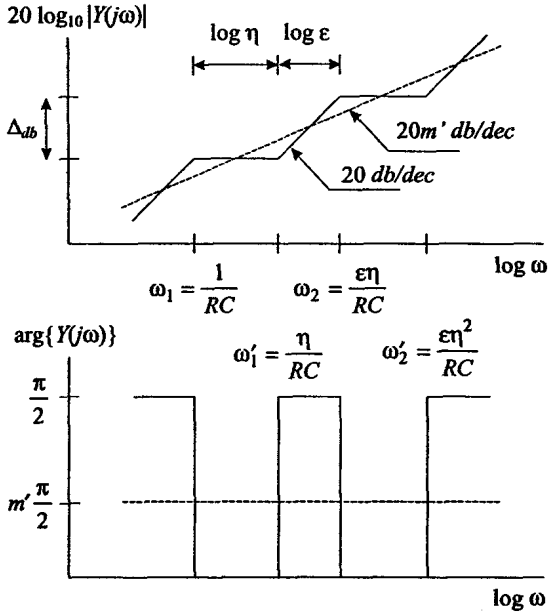

Fig. 2. Bode diagrams of $Y(j\omega)$.

Nevertheless, the implementation based on the Laplace definition (adopting the frequency domain) requires an infinite number of poles and zeros obeying a recursive relationship (Oustaloup, 1995). In a real approximation the finite number of poles and zeros yields a ripple in the frequency response and a limited bandwidth. Moreover, the digital conversion of the scheme requires further steps and additional approximations making difficult to analyze the final algorithm.

Based on the concept of fractional differential of order α, the Grünwald-Letnikov definition of a derivative of fractional order α of the signal $x(t)$, $D^{\alpha}x(t)$, leads to the expression:

$$D^{\alpha}x(t) = \lim_{h \to 0} \left\{ \frac{1}{h^{\alpha}} \sum_{k=0}^{\infty} \frac{\Gamma(k-\alpha)}{\Gamma(-\alpha)\Gamma(k+1)} x(t-kh) \right\} \qquad (5)$$

where Γ is the gamma function and h is the time increment. This formulation inspired a discrete-time calculation algorithm, based on the approximation of the time increment h through the sampling period T (Machado, 1997). A real implementation of (5) corresponds to a r-term truncated series, yielding the equation in the z domain:

$$\frac{Z\{D^{\alpha}x(t)\}}{X(z)} \approx \frac{1}{T^{\alpha}} \sum_{k=0}^{r} \frac{\Gamma(k-\alpha)}{\Gamma(-\alpha)\Gamma(k+1)} z^{-k} \qquad (6)$$

Clearly, in order to have good approximations, we must have a large r and a small T.

An important aspect of fractional-order controllers can be illustrated through the elemental control system represented in Fig. 3, with open-loop transfer function $G(s) = Ks^{-\alpha}$ ($1 < \alpha < 2$) in the forward path.

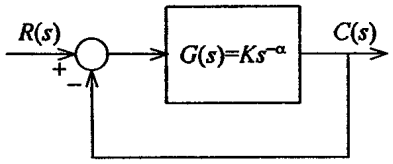

Fig. 3. Block diagram for an elemental feedback control system of fractional order α.

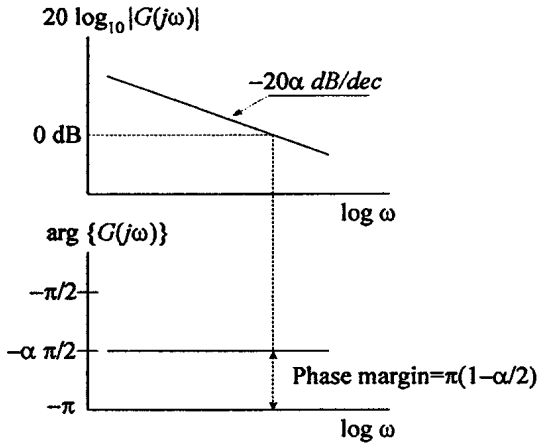

Fig. 4. Open-loop Bode diagrams of amplitude and phase for a system of fractional order $1 < \alpha < 2$.

The open-loop Bode diagrams (Fig. 4) have a slope of -20α *dB/dec* and a constant phase of $-\alpha\pi/2$ *rad*. Therefore, the closed-loop system has a constant phase margin of $\pi(1-\alpha/2)$ *rad*, that is independent of the system gain K.

3. DYNAMICS OF MECHANICAL SYSTEMS

In this section we study the adoption of fractional-order algorithms in the analysis of mechanical systems.

3.1 Describing Function Analysis of Systems with Backlash and Impact Phenomena

The standard approach to the backlash study is based on the adoption of a geometric model that neglects the dynamic phenomena involved during the impact process (Slotine and Li, 1991). Due to this reason often real results differ significantly from those predicted by that model.

In this section, we use the describing function (DF) method to analyse the phenomena of clearance without and with the effect of the impacts, usually called *static backlash* and *dynamic backlash*, respectively (Barbosa and Machado, 2002).

The static backlash model leads to a DF of a linear system of a single mass M_1+M_2 followed by the geometric backlash having as input and as output the position variables $x(t)$ and $y(t)$, respectively, as depicted in Fig. 5a.

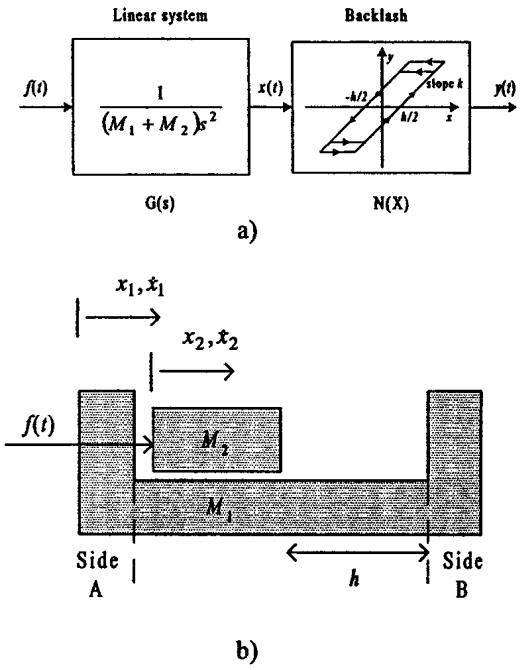

Fig. 5. System configurations: a) Static backlash; b) Dynamic backlash.

The describing function for $X > h/2$ is given by:

$$N(X) = \frac{k}{2}\left[1 - N_s\left(\frac{X/h}{1-X/h}\right)\right] - j\frac{2kh(X-h/2)}{\pi X^2} \quad (7a)$$

$$N_s(z) = \frac{2}{\pi}\left[\sin^{-1}\frac{1}{z} + \frac{1}{z}\cos\left(\sin^{-1}\frac{1}{z}\right)\right] \quad (7b)$$

For the *dynamic backlash*, the proposed mechanical model consists on two masses (M_1 and M_2) subjected not only to backlash but also to impact phenomena as shown in Fig. 5b.

A collision between the masses M_1 and M_2 occurs when $x_1 = x_2$ or $x_2 = h+x_1$. In this case, we can compute the velocities of masses M_1 and M_2 after the impact ($\dot{x}_1'$ and $\dot{x}_2'$) by relating them to the previous values ($\dot{x}_1$ and $\dot{x}_2$) through Newton's law:

$$(\dot{x}_1' - \dot{x}_2') = -\varepsilon\,(\dot{x}_1 - \dot{x}_2), \quad 0 \le \varepsilon \le 1 \quad (8)$$

where ε is the coefficient of restitution. In the case of a fully plastic (*inelastic*) collision $\varepsilon = 0$, while in the *ideal elastic* case $\varepsilon = 1$.

By application of the principle of conservation of momentum $M_1\dot{x}_1' + M_2\dot{x}_2' = M_1\dot{x}_1 + M_2\dot{x}_2$ and of expression (8), we can find the sought velocities of both masses after an impact:

$$\dot{x}_1' = \frac{\dot{x}_1(M_1 - \varepsilon M_2) + \dot{x}_2(1+\varepsilon)M_2}{M_1 + M_2} \quad (9a)$$

$$\dot{x}_2' = \frac{\dot{x}_1(1+\varepsilon)M_1 + \dot{x}_2(M_2 - \varepsilon M_1)}{M_1 + M_2} \quad (9b)$$

For the system of Fig. 5b we can calculate numerically the Nyquist diagram of $-1/N(F,\omega)$ for an input force $f(t) = F\cos(\omega t)$ applied to mass M_2 while considering as output position $x_1(t)$ of mass M_1.

The values of the parameters adopted in the subsequent simulations are $M_1 = M_2 = 1$ kg and $h = 10^{-1}$ m. Figures 6 and 7 show the Nyquist plots for $F = 50$ N and $\varepsilon = \{0.1, \ldots, 0.9\}$ and for $F = \{10, 20, 30, 40, 50\}$ N and $\varepsilon = \{0.2, 0.8\}$, respectively.

The Nyquist charts of Figs. 6–7 reveal the occurrence of a jumping phenomenon, which is a characteristic of nonlinear systems. This phenomenon is more visible around $\varepsilon \approx 0.5$, while for the limiting cases ($\varepsilon \to 0$ and $\varepsilon \to 1$) the singularity disappears. Moreover, Fig. 7 shows also that for a fixed value of ε the charts are proportional to the input amplitude F.

The validity of the model is restricted to an input force $f(t)$ with frequency higher than a lower-limit $\omega_C \approx [(2F/M_2h)^2(1-\varepsilon)^5]^{1/4}$ and lower than an upper-limit $\omega_L = 2(F/M_2h)^{1/2}$, corresponding to an amplitude of $x_1(t)$ within the clearance $h/2$. In the middle-range $\omega_C < \omega < \omega_L$ occurs a jumping phenomena at frequency $\omega_J \sim (F/M_2h)^{1/2}$.

Figure 8 illustrates the variation of the Nyquist plots of $-1/N(F,\omega)$ for the cases of the static and dynamic backlash and shows the log-log plots of Re{−1/N} and Im{−1/N} *vs.* ω for an input force $F = 50$ N and $\varepsilon = \{0.1, 0.3, 0.5, 0.7, 0.9\}$.

Comparing the results for the static and the dynamic backlash models we conclude that:

- The charts of Re{−1/N} are similar for low frequencies (where they reveal a slope of +40 dB/dec) but differ significantly for high frequencies;
- The charts of Im{−1/N} are different in all range of frequencies. Moreover, for low frequencies, the dynamic backlash has a fractional slope inferior to +80 dB/dec of the static model.

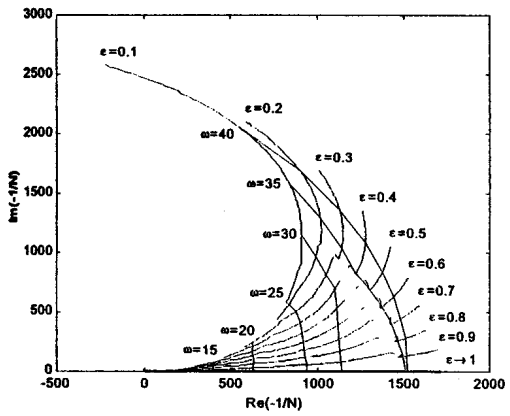

Fig. 6. Nyquist plot of $-1/N(F,\omega)$ for the dynamic backlash, $F = 50$ N and $\varepsilon = \{0.1, \ldots, 0.9\}$.

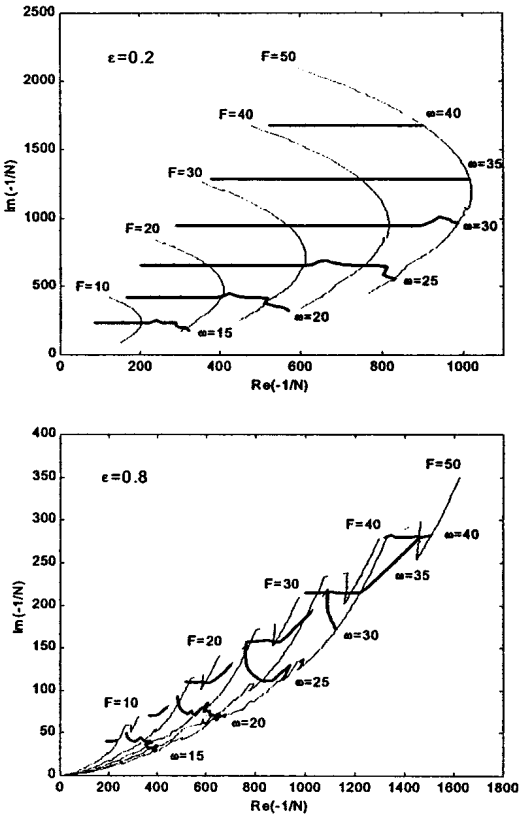

Fig. 7. Nyquist plots of $-1/N(F,\omega)$ for a system with dynamic backlash, $F = \{10, 20, 30, 40, 50\}$ N and $\varepsilon = \{0.2, 0.8\}$.

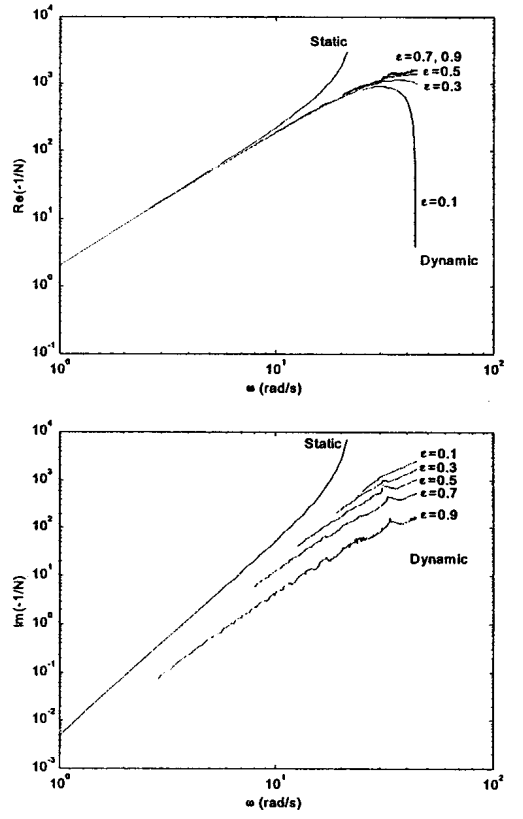

Fig. 8. Log-log plots of Re{−1/N} and Im{−1/N} *vs.* the exciting frequency ω, for $F = 50$ N and $\varepsilon = \{0.1, 0.3, 0.5, 0.7, 0.9\}$.

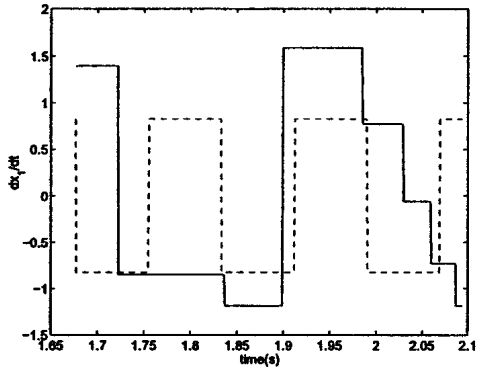

Fig. 9. Time response of the output velocity $\dot{x}_1(t)$ of the system with dynamic backlash, $F = 50$ N for $\omega = 20$ rad/s, $\varepsilon = 0.8$ (solid line) and $\omega = 40$ rad/s, $\varepsilon = 0.2$ (dashed line).

A careful analysis must be taken because it was not demonstrated that a DF fractional slope would imply a fractional-order model. In fact, in this study we adopt integer-order models for the system description but the fractional-order slope is due to continuous/discrete dynamic variation that results due to the mass collisions. In this line of thought, Fig. 9 shows the time response of the output velocity $\dot{x}_1(t)$ of a system with dynamic backlash for $\omega = \{20, 40\}$ rad/s and $\varepsilon = \{0.2, 0.8\}$ revealing that we can have either chaotic or periodic responses depending on the values of ω and ε.

3.2 Trajectory Control of Redundant Manipulators

A redundant manipulator is a robotic arm possessing more degrees-of-freedom (*dof*) than those required to establish an arbitrary position and orientation of the gripper (Fig. 10).

Redundant manipulators offer several potential advantages over non-redundant arms. In a workspace with obstacles, the extra *dof* can be used to move around or between obstacles and, thereby, to manipulate in situations that otherwise would be inaccessible.

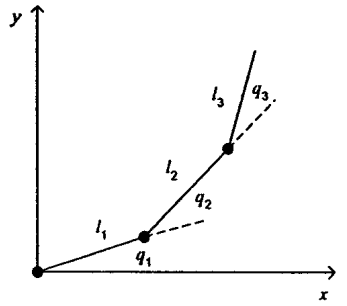

Fig. 10. The $3R$ planar redundant manipulator.

When a manipulator is redundant the inverse kinematics admits an infinite number of solutions. This implies that it is possible to induce a self-motion of the structure without changing the location of the gripper. Therefore, redundant manipulators can be reconfigured to find better postures for an assigned set of task requirements but, on the other hand, require more sophisticated control algorithms.

We consider a manipulator with n *dof* whose joint variables are denoted by $\mathbf{q} = [q_1, q_2, \ldots, q_n]^T$ and a class of operational tasks described by m variables $\mathbf{x} = [x_1, x_2, \ldots, x_m]^T$, $m < n$. The relation between the joint vector $\mathbf{q}$ and the manipulation vector $\mathbf{x}$ corresponds to the direct kinematics:

$$\mathbf{x} = f(\mathbf{q}) \tag{10}$$

Differentiating (10) with respect to time yields:

$$\dot{\mathbf{x}} = \mathbf{J}(\mathbf{q})\dot{\mathbf{q}} \tag{11}$$

Hence, from (11) it is possible to calculate a $\mathbf{q}(t)$ path in terms of a prescribed trajectory $\mathbf{x}(t)$. A solution in terms of the joint velocities is sought as:

$$\dot{\mathbf{q}} = \mathbf{J}^{\#}(\mathbf{q})\dot{\mathbf{x}} \tag{12}$$

where $\mathbf{J}^{\#}$ is one of the generalized inverses of the $\mathbf{J}$. The joint positions can be computed through the time integration of the velocities (12) according with the block diagram depicted in Fig. 11.

An aspect revealed by the algorithm is that repetitive trajectories in the operational space do not lead to periodic trajectories in the joint space. This is an obstacle for the solution of many tasks because the resultant robot configurations have similarities with those of a chaotic system (Duarte and Machado, 2002). To overcome this problem other alternatives methods for trajectory planning were proposed, namely by augmenting the Jacobian (so that it becomes of order $n \times n$) or by introducing optimization criteria.

We consider a $3R$ planar manipulators and, in this case, $\mathbf{J}$ has a simple recursive expression:

$$\mathbf{J} = \begin{bmatrix} -l_1 S_1 - l_2 S_{12} - l_3 S_{123} & \cdots & -l_3 S_{123} \\ l_1 C_1 + l_2 C_{12} + l_3 C_{123} & \cdots & l_3 C_{123} \end{bmatrix} \tag{13}$$

where l_i is the length of link i, $S_{ik} = \sin(q_i + q_k)$ and $C_{ik} = \cos(q_i + q_k)$. During the experiments it is considered $\Delta t = 0.001$ sec and $l_1 = l_2 = l_3 = 1$ m.

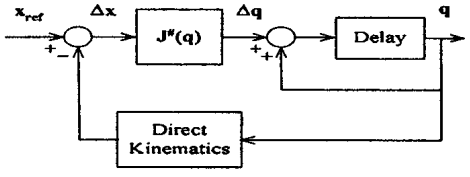

Fig. 11. Closed-loop trajectory controller with $\mathbf{J}^{\#}$.

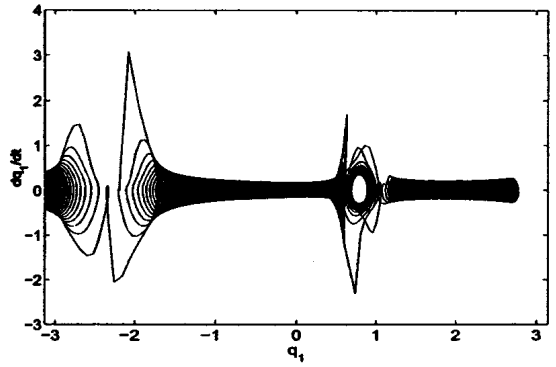

Fig. 12. Phase plane trajectory for the 3*R*- robot joint 1 at $r = 1$ m, $\rho = 0.1$ m, $\omega_0 = 3$ rad/s.

Figure 12 depicts the phase-plane joint trajectories for the 3*R*-robot, when repeating a circular motion with frequency $\omega_0 = 3$ *rad/sec*, center at $r = [x^2+y^2]^{1/2} = 1$ *m* and radius $\rho = 0.1$ *m* revealing position and velocity drifts, leading to different trajectory loops.

In order to characterize the frequency response we adopt two alternative exciting signals: a doublet-like and a white noise distributed throughout the 500-cycle of circular trajectories. For example, Fig. 13 depicts the resulting amplitude Bode diagrams for an exciting input superimposed on $x_{ref}(t)$:

$$Q_1(s)/X_{ref}(s) = K(s^{\alpha} + z)/(s^{\alpha} + p) \qquad (14)$$

where K is the gain, z and p are the zero and pole, respectively, and α is the zero/pole fractional order.

For the doublet excitation α takes integer values, namely $\alpha \approx 1.0$, in contrast with the case of white noise excitation where we get a fractional value $\alpha \approx 1.3$. This is due to the memory-time property of the fractional-order dynamics because it captures phenomena occurring during all the time-history of the experiment, in contrast with integer-order derivative that just captures the 'local' dynamics.

4. CONCLUSIONS

The theory of FC is still in a research stage but the recent progress in the area of chaos revealed promising aspects for future developments. In the field of automatic control systems some work has been carried out but the results are preliminary and further studies are required. This paper presented the fundamental aspects of the FC calculus, the main approximation methods for the fractional-order derivatives calculation and the implication of the FC concepts on the extension of the classical automatic control theory. Bearing these ideas in mind, several mechanical systems were described and their dynamics was analyzed in the perspective of fractional calculus. It was shown that fractional-order models capture phenomena and properties that classical integer-order simply neglect.

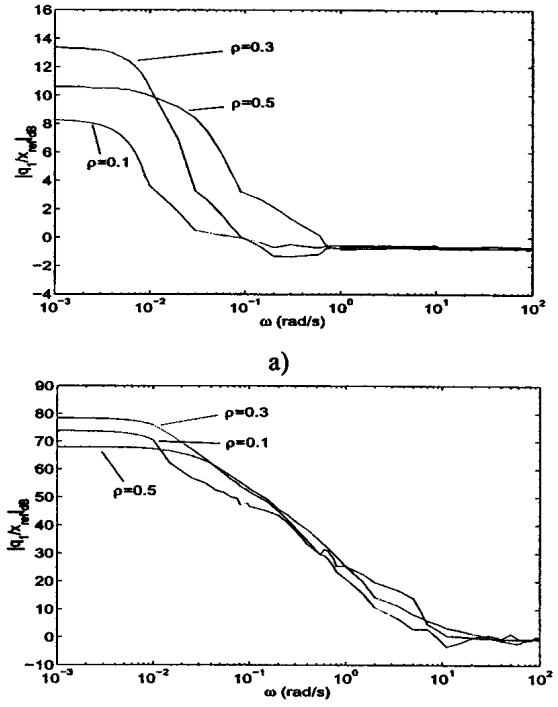

Fig. 13. Frequency response of the 3*R* robot, $\omega_0 = 3$ rad/s, $r = 2$ m, $\rho \in \{0.1, 0.3, 0.5\}$ m for a) A doublet-like; b) A white noise perturbation during all 500-cycle of circular trajectories.

REFERENCES

Barbosa, R. S. and J. T. Machado (2002). Fractional Describing Function Analysis of Systems with Backlash and Impact Phenomena. In: *Proc. of the 6th Int. Conf. on Intelligent Engineering Systems 2002*, pp. 521–526. Opatija, Croatia.

Duarte, F. and J. T. Machado (2002). Pseudoinverse Trajectory Control of Redundant Manipulators: A Fractional Calculus Perspective. In: *Proc. of the 2002 IEEE Int. Conf. on Robotics and Automation*, pp. 2406–2411 . Washington, USA.

Hilfer, R. (2000). *Aplications of Fractional Calculus in Physics*. World Scientific, Singapore.

Machado, J. A. T. (1997). Analysis and Design of Fractional-Order Digital Control Systems. *SAMS J. Syst. Analysis, Model., Simul.*, **27**, 107–122.

Machado, J. A. T. (2001). Discrete-Time Fractional-Order Controllers. *FCAA Fractional Calculus and Applied Analysis*, **4**(1), 47–66.

Miller, K. S. and B. Ross (1993). *An Introduction to the Fractional Calculus and Fractional Differential Equations*. Wiley, New York.

Oldham, K. B. and J. Spanier (1974). *The Fractional Calculus*. Academic Press, New York.

Oustaloup A. (1995). *La Dérivation Non Entière: Théorie, Synthèse et Applications*. Hermes, Paris.

Podlubny, I. (1999). *Fractional Differential Equations*. Academic Press, San Diego.

Slotine, J. E. and Li, W. (1991). *Applied Nonlinear Control*. Prentice-Hall, New Jersey.